

Blends of a longitudinal polymer liquid crystal with polycarbonate: relation of the phase diagram to mechanical properties

Witold Brostow*, Michael Hess† and Betty L. López‡

Departments of Materials Science and Chemistry, University of North Texas, Denton, TX 76203-5308, USA

and Tomasz Sterzynski

Ecole Européenne de Chimie des Polymères et des Matériaux, Louis Pasteur University, 4 rue Boussingault, F-67000 Strasbourg, France

(Received 5 June 1994; revised 16 August 1995)

This work is aimed at an evaluation of the capability to predict the mechanical behaviour of blends on the basis of the phase diagram. Connections between phase structures, the phase diagram and mechanical properties were studied for binary blends of polycarbonate (PC) based on bisphenol-A with PET/0.6PHB, where PET = poly(ethylene terephthalate), PHB = *p*-hydroxybenzoic acid and 0.6 = the mole fraction of PHB in the copolymer. PET/0.6PHB is a longitudinal polymer liquid crystal (PLC) with LC sequences in the backbone along the main-chain direction. The techniques used were differential scanning calorimetry (d.s.c.), thermomechanical analysis (t.m.a.) in the penetration and three-point-bending modes, thermally stimulated depolarization (t.s.d.) and two kinds of dynamic mechanical analysis (d.m.a.) as a function of frequency ω and temperature T . The resulting phase diagram is plotted as a quasi-binary one (T versus concentration of PET/0.6PHB or PC) but provides information on miscibilities of all three pairs of constituents; it contains equilibrium as well as long-living non-equilibrium phases, including the quasi-liquid. D.s.c. and d.m.a. results show that glass transition temperatures for the PC-rich phase drop by $\sim 50^\circ\text{C}$ after 1 h of annealing, with evident consequences for mechanical properties. Variations of storage modulus and strain as a function of time are reported for different blend compositions. Isothermal storage moduli and results of three-point bending as a function of composition are connected to the phase diagram. Prediction of mechanical behaviour is possible from miscibilities of constituents in specific regions of the diagram. Copyright © 1996 Elsevier Science Ltd.

(Keywords: polymer blends; polymer liquid crystal; polycarbonate)

INTRODUCTION

Most so-called engineering polymers (EPs) consist of flexible chains, which imposes definite limits on their mechanical performance. These limits can be exceeded in at least three ways. One way consists of the introduction of reinforcements, such as graphite or glass fibres into an epoxy. The resulting class of materials has been called macroscopic composites¹ or else heterogeneous composites²; we shall use the latter name. On occasions the use of heterogeneous composites causes serious problems: insufficient adhesion between the fibre and the matrix leads to debonding and pull-out of individual fibres and to delamination of entire layers in layered structures. The second way out consists of making so-called molecular composites, in which rigid polymer

molecules are dispersed between flexible chains^{3,4}. The difficulty here is in processing of the rigid polymers, which typically are soluble only in highly corrosive solvents. There is also a third way: using polymer liquid crystals (PLCs) in which every chain contains reinforcing LC sequences along with flexible sequences.

The advantages of PLCs are numerous, and have been discussed before^{5–8}. However, PLCs have also a disadvantage: they are typically more expensive than EPs. Hence the idea of blending PLCs with EPs, so that the advantageous properties of a PLC are preserved in the blend, while the price is distinctly lower than that of the respective pure PLC. The idea is not new, and various attempts to implement it have been reported^{9–24}. However, PLCs typically form several phases^{2,25–27}, and so do PLC-containing blends. By definition of PLCs, at least one LC phase has to appear. Sometimes there are several such phases, while we have discovered in PLC systems a new phase called the quasi-liquid^{28–30}. Since a PLC is usually a copolymer, we have three constituents in a blend. The miscibilities—or otherwise—of the three pairs of constituents determine the capability to achieve

* To whom correspondence should be addressed

† Also at: FB-6 Physical Chemistry, Gerhard Mercator University, 47048 Duisburg, Germany

‡ Also at: Department of Chemistry, University of Antioquia, Apartado Aéreo 1226, Medellín, Colombia; and Colciencias, Bogotá, Colombia

blended materials with properties better than those of the components. Since the miscibilities depend on the temperature and composition, the phase diagram is needed. There is a statistical mechanical theory of PLCs created by Flory^{31–33}, and then extended by Matheson^{34,35} and by us^{36–38}. The theory makes possible predictions of the clearing (isotropization) temperatures as a function of LC concentration and molecular structures. For the remainder of the phase diagram, experiments are needed. Given the full phase diagram, we would like to find out whether indeed the mechanical properties can be predicted from it. The phase diagram for the blends must take into account the diagram for the respective pure PLC in which the concentration x of LC sequences in a series of copolymers is the independent variable.

The PLC used in this study was PET/0.6PHB, where PET is poly(ethylene terephthalate), PHB is *p*-hydroxybenzoic acid, and 0.6 the mole fraction of the LC constituent (PHB) in the copolymer; for brevity we shall often use the abbreviation COP for PET/0.6PHB. The LC sequences are in the backbone along the main-chain direction, hence COP is a *longitudinal* PLC^{5,7,8}. COP has already been studied by a variety of techniques; a companion paper in this journal presents its melt rheological behaviour and morphology³⁹. Essential for the success of our undertaking was the fact that the phase diagram of the PET/ x PHB copolymers as a function of x was already established³⁰ on the basis of results reported in 18 publications. As for the EP, we have decided to use polycarbonate, to be denoted in the following as PC. Since the present team spans four countries, we had the capability to check results obtained in any laboratory by conducting analogous experiments on identical samples elsewhere.

EXPERIMENTAL

Material preparation and processing

COP was obtained from Eastman Kodak, Kingsport, TN, as well as from Unitika Ltd, Kyoto, Japan (LC-3000). PC was produced by Bayer AG, Leverkusen, Germany (Makrolon 2800). The former has been characterized in earlier papers^{2,28,30,40,41}. The properties of the latter are as follows: density $\rho = 1.20 \text{ g cm}^{-3}$; melt flow index ($MFI \text{ 300/11.8}$) = 7 g/10 min; stress at yield $\sigma_y = 65 \text{ J cm}^{-3}$; modulus of elasticity in tension $E = 2300 \text{ J cm}^{-3}$; and elongation at fracture $\epsilon_f = 110\%$. We recall that $1 \text{ J cm}^{-3} = 1 \text{ MPa} = 1 \text{ MN m}^{-2}$ exactly. Moreover, $1 \text{ MPa} = 145.038 \text{ psi}$. All samples we have studied—at any location—had the same basic thermal history.

To exclude possible degradation by hydration, the components were dried in a vacuum drier as follows: COP for 8 h at 130°C; PC for 6 h at 125°C. Blending was done in Strasbourg in a single-screw Goettfert extruder with screw diameter 20 mm and length-to-diameter (L/D) ratio = 20. Extrusion was performed at the following conditions: barrel temperature, 230–260–270°C; screw speed, 40 rev min⁻¹; residence time, ~2 min. The extruded rod, of approximately 3 mm in diameter, was granulated using a pelletizing unit.

Most samples for mechanical testing and all for microscopic observations were produced by injection moulding in the form of plates with a thickness of

2 mm. The injection moulding was performed under the following conditions: temperatures in the barrel, 270–280–290–300°C; mould temperature, 100°C; filling pressure, 130 J cm⁻³; packing pressure, 46 J cm⁻³; packing time, 10 s; cooling time in the mould, 10 s.

To determine the influence of orientation on mechanical properties, samples were cut parallel as well as perpendicular to the flow direction. Certain samples were prepared in the solid state but in the temperature range 210–220°C by compression lasting either 10 or 60 min. Additionally, we also obtained blend samples by co-precipitation from a common solution of 20 vol% trifluoroacetic acid and 80% chloroform. The precipitating agent was acetone. The samples were dried overnight under vacuum and subsequently annealed with and without applied pressure for specified periods of time.

Characterization and testing

Differential scanning calorimetry (d.s.c.). The blends were investigated with two Perkin–Elmer apparatuses (DSC-7 in Denton and DSC-2 in Duisburg). The samples were encapsulated in sealed Al pans and run in an atmosphere of dry N₂. The heating rate was always 20 K min⁻¹. Calibrations were performed with certified standards of In and Zn. The transition temperatures reported in the following constitute averages from three to five samples.

Thermal mechanical analysis (t.m.a.) T.m.a. studies were performed with two Perkin–Elmer apparatuses (TMA-7 in Denton and TMA-2 in Duisburg) in the penetration mode in a He atmosphere for temperatures up to 320°C in Denton and up to 240°C in Duisburg. The heating rate used was 10 K min⁻¹ both instances. The apparatus in Duisburg was also used for three-point bending, following the German standards DIN 53452 and DIN 53457.

Dynamic mechanical analysis (d.m.a.) D.m.a. was performed in Denton on rectangular strips (8.0 × 8.0 × 1.5 mm) in the bending mode with a Polymer Laboratories MK II apparatus using cantilever clamping geometry. An isothermal scan over several decades of frequency led to the choice of frequencies for the heating scans. The latter were performed for frequencies $\omega = 1.0, 3.0$ and 10.0 Hz in the temperature range from –100°C to +200°C. The heating rate was the same in all runs and equal to 2 K min⁻¹. D.m.a. measurements were also performed in Duisburg in the torsional pendulum mode with an ATM-3 apparatus of Firma Myrenne from –180°C to +300°C in the ω range from 0.1 to 10.0 Hz. That apparatus is based on a construction of Illers and Breuer⁴²; a torsional force is applied and the free decay is determined at a constant frequency.

Since the heating rates in d.s.c., t.m.a. and d.m.a. were different, glass transition temperatures of pure PET were compared. All three methods gave $T_{g,PET} = 75^\circ\text{C}$, in agreement with earlier results³⁰.

Tensile properties. The elastic modulus, proof stress point, tensile strength and percent elongation at yield and at break were determined in a fully computerized

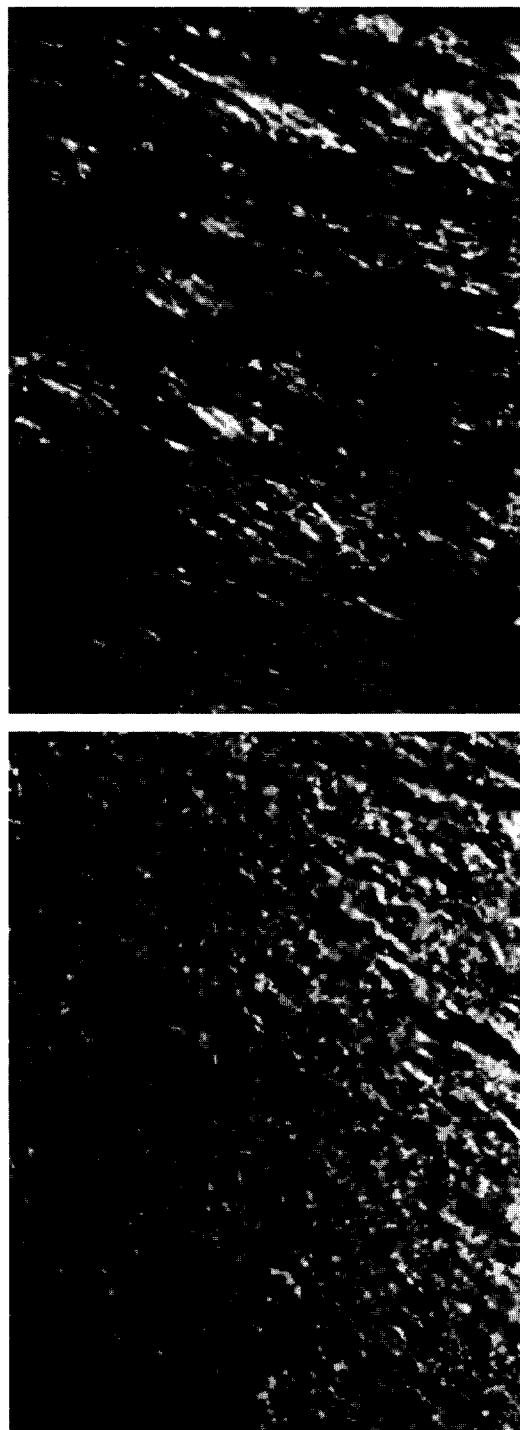


Figure 1 The morphology of PC + COP blends containing 20 wt% COP. Top, a near-to-the-wall part of the section with a diagonal length of 750 μm ; bottom, the middle part with the same diagonal

SINTECH universal testing machine in Denton. The specimens were prepared in Strasbourg according to ASTM Standard D638M, version M-II.

Morphology. Studies were performed on films of 10 μm thickness cut from the specimens with a Leica microtome. The films were obtained from the centres (half of the thickness) and from the near-to-wall regions of injection-moulded specimens and then placed between glasses of a Nikon Optiphot microscope with a polarizing head.

MORPHOLOGY

Microscopic studies of morphology were conducted for pure PC and for blends containing 5, 10, 15 and 20 wt% COP. For brevity we show only micrographs for the last composition in *Figure 1*.

Inspection of the micrographs shows that shear flow, particularly in the near-to-wall regions of the injection-moulded specimens, causes the formation of LC-rich fibrils in an LC-poor matrix. The effect becomes more and more pronounced when the concentration of the COP increases. When moving from the wall region towards the centre, that is from shearing to elongational flow, the fibrils gradually become closer to spherical in shape. Such LC-rich, nearly-spherical islands were found by scanning electron microscopy (SEM) in the solid blends of our COP with PET². The specimens subjected to mechanical testing contain both the fibrils and the islands, with a gradual transition between the two shapes—as necessarily encountered in components made from our blends for any specific applications.

The formation of islands in the melt can be explained by differences of the viscosity of LC-poor and LC-rich phases. Our LC-poor matrix contains high amounts of PC. As demonstrated in the companion paper³⁹, the melt viscosity of the matrix is much higher than that of COP. The shear flow of the high viscosity matrix together with the interfacial interaction causes deformation of the islands in the melt, and consequently formation of the fibril structures. Fibrils were considered in a qualitative model of hierarchical structures in PLCs by Sawyer and Jaffe⁴³. By contrast, in the elongational flow in the centre of the conduit no such deformation takes place; the islands are able to undergo relaxation and acquire their nearly spherical shape dictated by the interfacial tension. Moreover, the lack of shearing in the centre results in a relatively homogeneous distribution of the low viscosity islands in the high-viscosity matrix. The structure of the islands was elucidated before on the basis of SEM and wide-angle X-ray scattering (WAXS) performed in HASYLAB at DESY, Hamburg, in connection with formation of hierarchical structures²⁹. Rules of formation of such structures were formulated in terms of homeomorphism—or lack of it—of the building blocks. Viewing the fibrils and the islands in *Figure 1*, we recall Rule 5: assembling the building block entities in a specified way one can achieve properties which a system of *unassembled* entities does not have.

CALORIMETRY OF THE BLENDS

Since thermal history and mechanical treatments are known to influence thermophysical properties, we have determined first glass transition temperatures T_g of the PC-rich phases of blend specimens of varying compositions and prepared in a variety of ways. The results are shown in *Figure 2*.

Inspection of *Figure 2* shows, first of all, that samples of the same composition can have glass transition temperatures varying from ~ 100 to 150°C , depending on the preparation procedure. This is another and important dimension of our intelligent processing approach: while at this stage we have at our disposal only glass transitions and not yet the entire phase

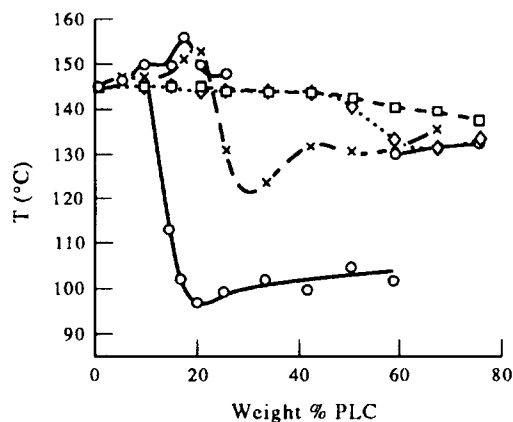


Figure 2 Glass transition temperatures T_g of PC + COP mixtures: -----, blends prepared in the solid state by compression for 10 min at 210–220°C under the pressure $P = 4.0 \text{ J cm}^{-3}$; ·····, blends prepared by precipitation from solution and subsequent compression at $P = 0.1 \text{ J cm}^{-3}$ for 10 min at 210–220°C; - · - ·, blends prepared by precipitation from solution and compression at $P = 4.0 \text{ J cm}^{-3}$ for 1 min at 210–220°C; —, blends prepared by precipitation from solution and compression at $P = 4.0 \text{ J cm}^{-3}$ for 60 min at 210–220°C

diagram, we have acquired a powerful tool for manipulating mechanical properties for a fixed composition.

Figure 2 shows us also that longer annealing times correspond to lower glass transition temperatures, apparently as a consequence of more intimate mixing at elevated temperatures. To confirm or reject this supposition, samples were prepared by precipitation from solution and compression at $P = 4.0 \text{ MPa}$ for several hours at 210–220°C. The resulting curves of T_g versus composition were indistinguishable from the curve for 60 min annealing shown in the figure⁴⁴.

Finally, Figure 2 also confirms earlier statements about the necessity of taking into account non-equilibrium phases and their transitions^{7,30}. Two new kinds of graphical representations of the non-equilibrium phases were proposed in ref. 7. These statements are also supported by the results of Springer and co-workers for PLC combs, showing the formation of *metastable but reproducible* phases⁴⁵ as well as polymorphism of LC phases^{46,47}.

PHASE DIAGRAM

Techniques described in the Experimental section were used to determine the phase diagram of the PC + COP system. The starting point was the part of the phase diagram of PET/ x PHB copolymers reported in ref. 30 for $x = 0.6$. Given the amount of work invested then in coordinating results from laboratories around the world, choosing the most reliable ones which additionally were confirmed by our own, this dramatically facilitated the present undertaking.

Construction of the diagram involved the comparison of transitions recorded by various techniques. The most reliable technique turned out to be t.m.a., confirming our conclusions reached elsewhere³⁰: i.e. then, as well as for the blends now studied, there are some transitions which are difficult to locate by d.s.c. This is also the reason for the use of several other techniques. Both forms of d.m.a. we have used as well as t.s.d. are more sensitive than d.s.c., while t.m.a. is the most sensitive. By 'sensitivity' we mean here not only the appearance of a transition,

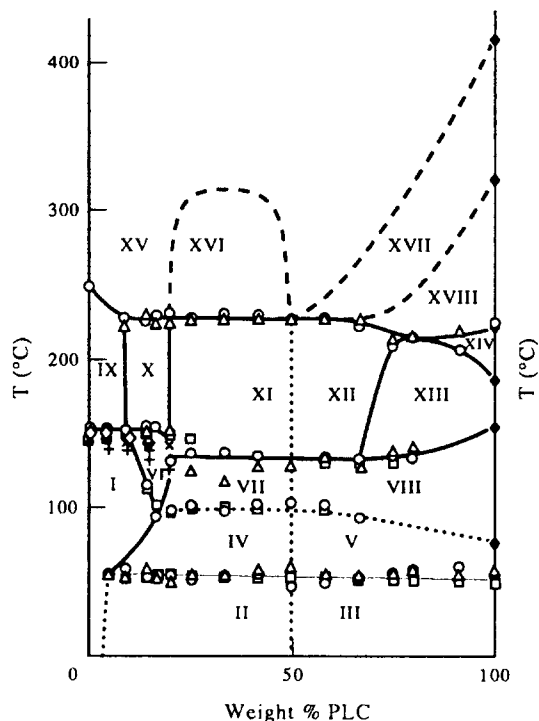


Figure 3 Phase diagram of the PET/0.6PHB (=COP) + PC system. Symbols: Δ , d.s.c. results for samples precipitated from solution and annealed for 60 min; \circ , d.m.t.a. results for the same samples; \square , t.m.a. results for the same samples; \diamond , d.s.c. results for samples obtained by compression without annealing; \times , d.m.t.a. results for the same samples; +, t.m.a. results for the same samples. Lines: -----, hypothetical lines (not enough experimental points); ·····, transitions both at and in the region surrounding a line (as in cold crystallization or island formation). Terminology: i-l, isotropic liquid; q-l, quasi-liquid; cr, crystal; isl, island (rich in LC); sm, smectic; (y), low concentration of y in comparison to the other phases present. The regions in the diagram marked with Roman numerals contain the following phases: I = PC cr, PC-rich glass (PC glass); II = PC cr, PC glass, PET glass; III = (PC + PHB) glass, PET glass, PHB-rich isl (PHB isl); IV = PC cr, glass, q-l, small amounts of PET cr; V and VIII = glass, q-l, PHB isl, PET cr; VI = glass, q-l, PC cr; VII = glass, q-l, PC cr, PET cr; IX = PC cr, i-l; X = PC cr, q-l, i-l; XI = PC cr, q-l, i-l, PET cr; XII = PC cr, q-l, PHB isl, PET cr XIII = q-l, PHB isl, PET cr; XIV = sm E, i-l; XV = i-l; XVI = (PC + PET)-rich liquid, PHB-rich liquid; XVII = i-l, sm B; XVIII = i-l, sm E, sm B

but also a relatively narrow width of the respective peak (in d.s.c. the peaks are often fairly broad). Any transition detected and located by other techniques has shown up in t.m.a. as well. By their nature, transitions involving LC phases cause smaller enthalpic and entropic effects than, for instance, melting from a crystal into an isotropic phase. Thus, we do not recommend basing phase diagrams for systems including PLCs on one technique alone. However, if time does not permit to use several techniques, then t.m.a. would be our method of choice. At the same time, we reiterate the fact noted elsewhere³⁰ that the resolution of neighbouring signals and their peak width is technique-dependent. The procedures used to arrive at a reliable phase diagram have been described in ref. 30 and again in a dissertation⁴⁸. In the present work we also have the advantage of experiments conducted in different laboratories and on samples of the same composition but from two sources (Eastman Kodak, Unitika) and comparing the results.

The phase diagram resulting from the use of all techniques named, from data obtained in Denton as well as in Duisburg, is presented in Figure 3. Inspection of

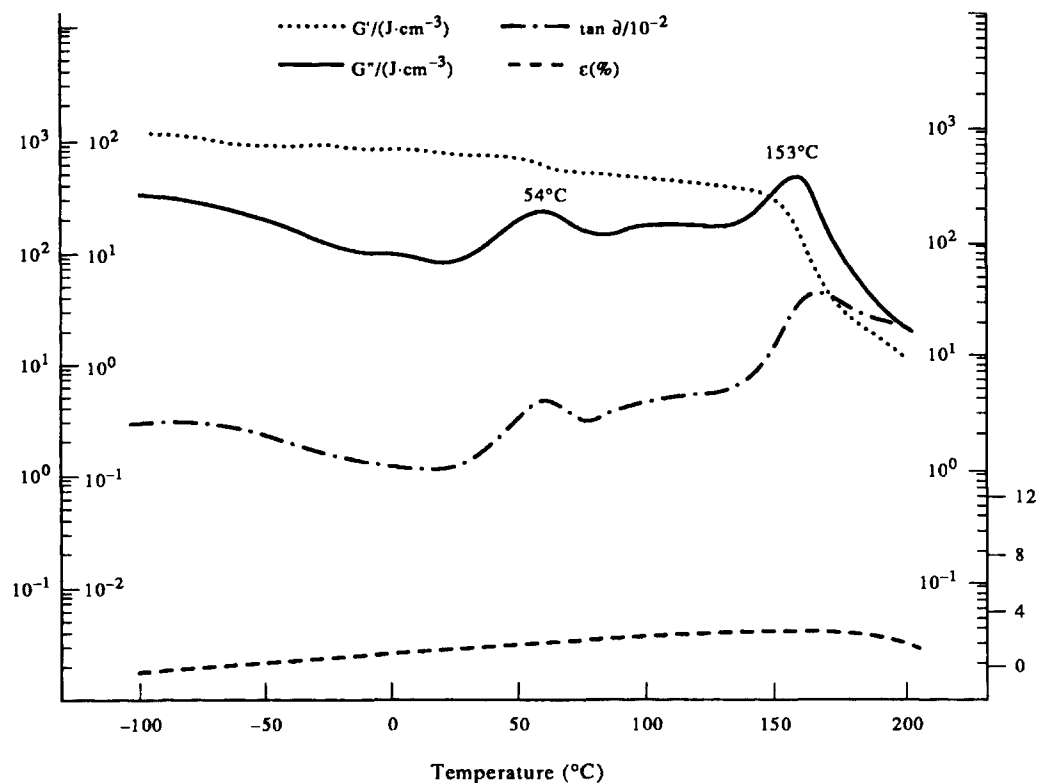


Figure 4 Pendulum d.m.t.a. results for a blend containing 20 wt% COP obtained from solution by acetone precipitation and kept in compression for 1 min at 210–220°C under $P = 4.0 \text{ J cm}^{-3}$. $\omega = 1.0 \text{ Hz}$

the diagram shows, first of all, a multiplicity of phase transitions—which is why we have 18 phase regions. Except for the isotropic liquid, all other regions contain several phases, with the most complex containing four phases. Since we are including non-equilibrium phases, the Gibbs phase rule is not being violated. There are two LC phases, smectic E and smectic B, as found by Yoon and co-workers⁴⁹; previous work³⁰ as well as the current study establish agreement of the locations of phase transitions as determined by Yoon *et al.* with other investigations including our own.

We recall the definition of the quasi-liquid (q-l)^{28–30}: a phase between the glass and melting transitions, with low mobility and retarded response to the application of external forces. Low mobility distinguishes q-l from an ordinary liquid which flows much more readily. The retarded mechanical response is similar to that in the leathery state of elastomers; see for instance ref. 50. Our q-l originates from PET glass, and it is in q-l that cold crystallization of PET occurs; the dotted nearly horizontal line in Figure 3 around 100°C indicates the maximum intensity of cold crystallization. Above that line we have more PET crystals, as shown in the full phase diagram for PET/*x*PHB copolymers³⁰.

The vertical dotted line around 50 wt% COP represents the formation of LC-rich islands in the LC-poor matrix. We have already discussed the island formation in the Morphology section in terms of conditions prevailing during melt flow. The islands are created in a kinetic process, their appearance depending not only on the composition and temperature but also on the previous mechanical and thermal history of the sample. Thus, island formation occurs also to the left of the dotted line in question, but compositions closer to pure

PC require more time for the islands to appear. The dotted line corresponds to the maximum of island formation. This fact is also reflected in mechanical properties, as discussed in the following section.

There exists a thermodynamic condition (corresponding to infinite formation time), namely the lowest LC concentration $\theta_{\text{LC limit}}$ below which at given temperature T and pressure P an LC island will not form. We have mentioned above the statistical mechanical theory of PLC phases developed by Flory^{31–33}, expanded by Flory and Matheson^{34,35}, and amplified further by us^{36–38}. We expect that continuing work on this theory will be able to render an analytical expression for $\theta_{\text{LC limit}}$ and also to predict transitions which are experimentally inaccessible (thermal degradation or chemical reactions taking place at the transition temperatures). It is important to note that $\theta_{\text{LC limit}}$ manifests itself in the mechanical behaviour; see below.

Region XVI in the phase diagram is hypothetical; we do not have experimental points at such high temperatures. As discussed below in the next section, above 290°C transesterification reactions are possible, hence the components to which our diagram pertains can exist for a limited time only. There are several reasons for the inclusion of this region. First, it represents a natural continuation upwards of the borders between regions X and XI and also XI with XII. Second, as discussed above, we have at lower temperatures the islands dominated by PHB. Now, at higher temperatures, PHB will separate even more easily, leaving a PC-rich phase outside. Since PC and PET both consist of flexible sequences and we are now in molten phases, PET sequences will try to get into the PC-rich phase. Third, there is evidence from the companion work on melt rheology³⁹ that the blends at 290°C containing 20% PLC—just inside the two-phase

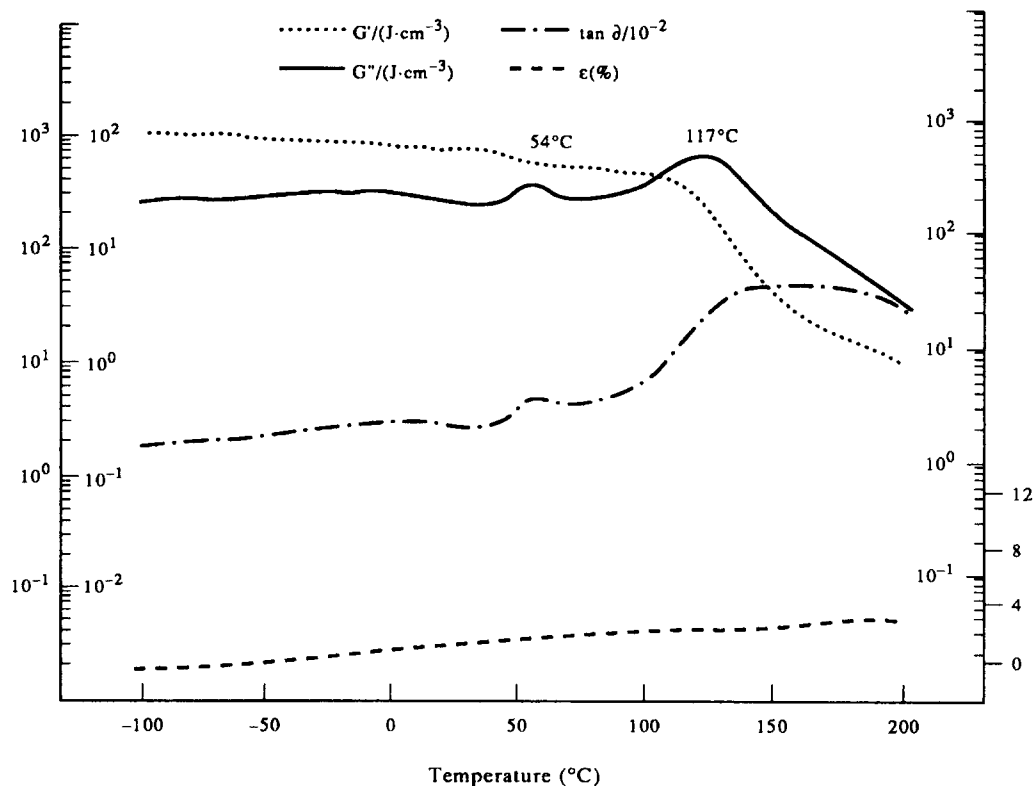


Figure 5 Results as in Figure 4, but for a material annealed for 10 min

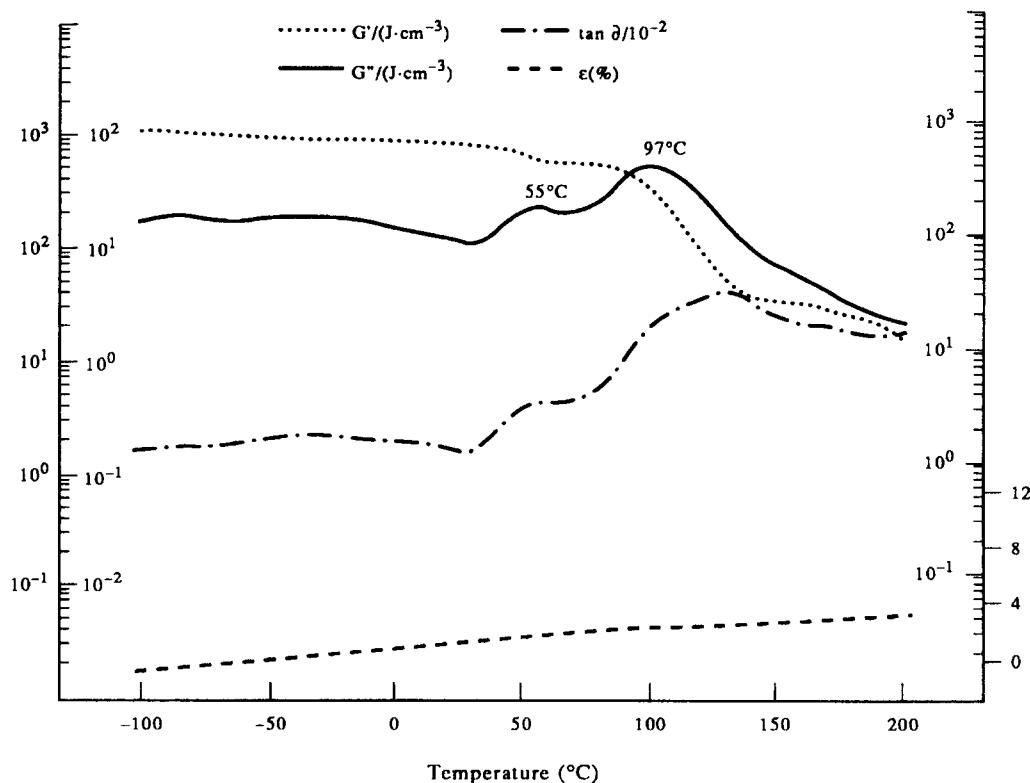


Figure 6 Results as in Figure 4, but for a material annealed for 60 min

region XVI—behave differently from those with 15% PLC. This is understandable, since our diagram shows the latter composition inside the one-phase region XV.

Finally, except for the strong dependence on the preparation procedures of the glass transitions of the

PC-dominated phases (discussed separately in the preceding section), we observe a gratifying agreement of temperatures of phase transitions determined by different techniques and/or at different laboratory locations. Except for the hypothetical phase region XVI just

discussed, the other phase transitions shown in *Figure 3* are found repeatedly and reproducibly. The phase diagram will be also used in the next section to explain earlier controversies about the miscibility of PC with COP—or, more accurately, to eliminate the root of these controversies.

MECHANICAL PROPERTIES

D.m.a. results have already been used to locate transitions for the phase diagram in the preceding section. In view of the d.s.c. results discussed under the heading Calorimetry, we have also used d.m.a. to study effects of sample history on phase transitions. Some results pertaining to these effects obtained with the pendulum d.m.t.a. are shown in *Figures 4–6*. The moduli shown are related by the standard equation

$$G^* = G' + iG'' \quad (1)$$

where G^* is the complex modulus, G' the storage modulus and G'' the loss modulus. $\tan \delta = G''/G'$ is shown in the same figures, as is the corresponding strain ϵ .

Comparison of *Figures 4–6* shows that there is a dramatic fall of the glass transition temperature of PC with time: from 153°C after 1 min to 117°C after 10 min and then to 97°C after 1 h. This fully confirms the d.s.c. results. We know from the phase diagram that PET is virtually immiscible with PC. We also know that transesterification reaction is possible, but ^{13}C nuclear magnetic resonance (n.m.r.) spectroscopy shows that it requires time, and measurable effects are observed at $T \geq 270^\circ\text{C}$ ⁵¹. Even more importantly, transesterification results in a random statistical distribution of segments of different types. Guan *et al.*⁵² have prepared several PET/*x*PHB samples and found by ^1H n.m.r. at 400 MHz that specimens kept at 270°C do not show random distribution of PET and PHB sequences; only those kept at 290°C are approaching that distribution. Therefore, the observed fall of T_g from 153°C to $\sim 100^\circ\text{C}$ can only be explained by gradual mixing of PC with PHB. Kyu and Zhuang⁵³—who have previously dealt with the same system—noted that there is controversy in the literature, since some sources claim that PC and PET/0.6PHB are immiscible. By optical microscopy they concluded that there is miscibility. Since PET/0.6PHB forms at least two phases by itself, statements that it is ‘miscible’ or ‘immiscible’ with PC can only describe part of the situation. Pairwise miscibilities PC + PET and PC + PHB have to be taken into account, and here seems to lie the root of earlier controversies. Consequences of the miscibility of PC with PHB for our capability to conduct intelligent processing and manipulate properties were already noted above.

To see the effects of time t and composition on viscoelastic properties, we have studied effects of time on the storage modulus G' and on the strain ϵ . Two types of behaviour were observed. For blends containing relatively low concentrations of PC, G' decreased as a function of time, while ϵ increased until reaching a plateau. An example of this type of behaviour is shown in *Figures 7 and 8*. The results in *Figure 7* can be explained by the *coalescence* of the islands with time. A smaller number of the islands resulted in less reinforcement and hence the fall of the storage modulus; see also the discussion of *Figure 11* in the following section. Given

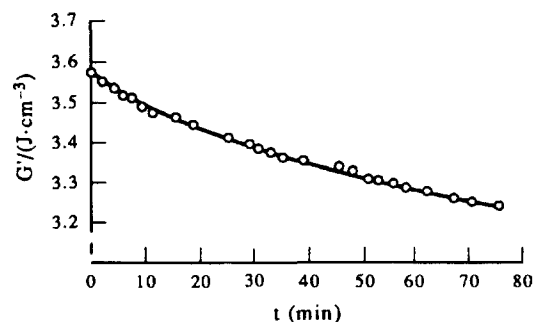


Figure 7 Variation of the storage modulus G' with time t for a blend containing 75% COP obtained by precipitation from solution and annealed under compression $P = 4.0 \text{ J cm}^{-3}$ for 1 min at 210–220°C. Pendulum d.m.t.a. results for $\omega = 1.0 \text{ Hz}$ at 173°C

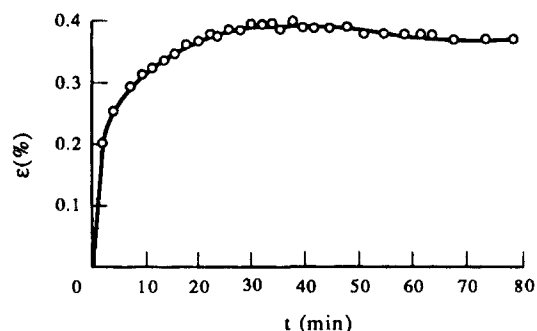


Figure 8 Variation of strain ϵ with time t for the same specimen as in *Figure 7*

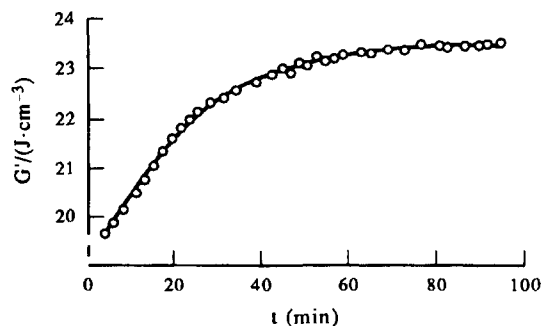


Figure 9 Variation of the storage modulus G' with time t for a blend containing 50% COP obtained by precipitation from solution and annealed under compression $P = 4.0 \text{ J cm}^{-3}$ for 1 min at 210–220°C. Pendulum d.m.t.a. results for $\omega = 1.0 \text{ Hz}$ at 173°C

the temperature of the experiment, the coalescence would occur also without a sinusoidal force (an annealing process), but to a somewhat smaller extent. While the angle of torsion is small, the sinusoidal force helps the coalescing islands to surmount the surface tension. Given the relatively low concentration of PC, its crystallization was difficult and did not affect the modulus.

By contrast, when the PC concentration was relatively high, G' increased with time while the strain decreased. This type of behaviour is shown in *Figures 9 and 10*, and can be explained by an increase in the degree of crystallinity of PC with time, resulting in densification and shrinking of the material. The crystallinity increase was visible in d.s.c. curves and also in WAXS determined before and after pendulum d.m.t.a. determination, but we do not include the respective curves for brevity. It

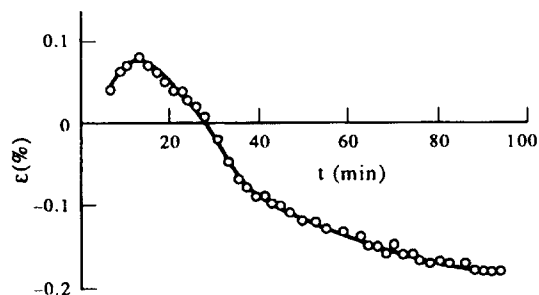


Figure 10 Variation of strain ϵ with time t for the same specimen as in Figure 9

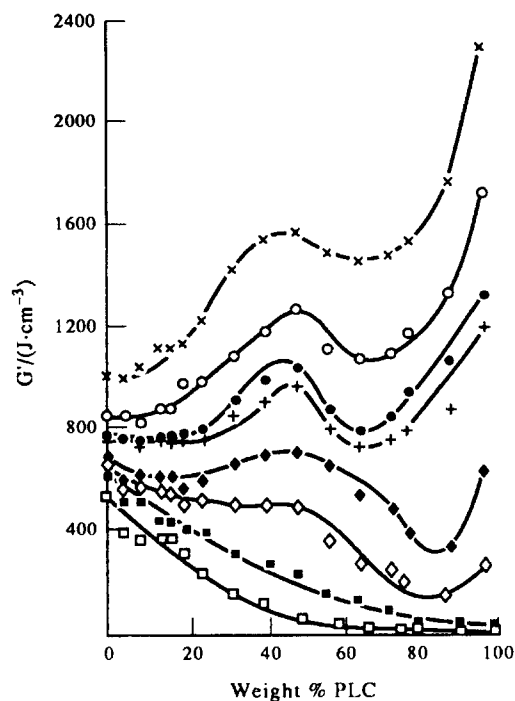


Figure 11 Storage modulus as a function of composition determined at: \times , -100°C ; \circ , -50°C ; \bullet , 0°C ; $+$, $+20^{\circ}\text{C}$; \blacklozenge , $+50^{\circ}\text{C}$; \diamond , $+60^{\circ}\text{C}$; \blacksquare , $+100^{\circ}\text{C}$; \square , $+140^{\circ}\text{C}$

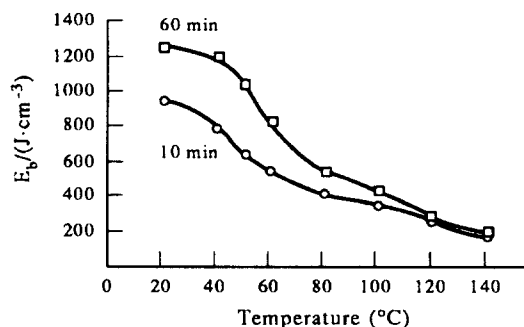


Figure 12 Bending modulus E_b of blends containing 50 wt% COP determined with pendulum d.m.t.a. as a function of temperature and sample preparation. The samples were obtained by precipitation from solution and annealed under the compression $P = 4.0\text{J cm}^{-3}$ at $210\text{--}220^{\circ}\text{C}$ for either 10 or 60 min

appears that the degree of crystallinity of PC is enhanced by the presence of COP. We recall the result of Takayanagi *et al.*³⁴: in blends of two polyamides, one aromatic and one aliphatic, the rigid chains act as a nucleating agent for the crystallization of the flexible

matrix. In our case, PC alone is rather amorphous and tricks have to be applied (penetration by vapours of acetone or tetrahydrofuran) to induce its crystallization.

We have also performed mechanical testing in tension and in three-point bending. The former were performed in the concentration range from 0 to 20 wt% COP, the latter in the entire concentration range. Given the limited range of tensile testing, for brevity we do not include the results here, but they can be found in ref. 48. Because of a striking direct connection of three-point bending results to the phase diagram, we now discuss these results separately in the last section.

THE PHASE DIAGRAM-PROPERTY CONNECTION

We return now to d.m.a. results, and show in Figure 11 the storage modulus G' as a function of concentration along several isotherms. Except for the two highest temperatures which are above all glass transitions, other curves show a maximum at ~ 50 wt% PLC. Starting from the pure PC side, we first observe, at low temperatures in particular, relatively flat regions. The plateaux correspond to LC concentrations below $\theta_{\text{LC limit}}$, so that LC-rich islands are not formed, hence there is no reinforcement effect. Above $\theta_{\text{LC limit}}$ we have gradual formation of the islands, which is reflected in the increase of the storage modulus. The modulus has a maximum at 50%; above that concentration a phase inversion takes place; see the central dotted line in the phase diagram (Figure 3). Hence the number of islands decreases, and it is the number and shape of the reinforcing regions and not their total volume that maximizes the reinforcement; this is known in general⁵⁵ and also has been specifically confirmed by molecular dynamics computer simulations for PLCs⁵⁶. 'Eating up' of smaller islands by larger ones when increasing the PLC concentration θ has been observed by SEM in our study of the same COP with PET². In that system the phase inversion taking place with increasing θ also had consequences for mechanical properties of the blends. Increasing θ further, we observe completion of the phase inversion, occurring at low temperatures at approximately 70% COP (if our PLC consisted of pure PHB, the completion of phase inversion would have to occur near to 50% PLC). Afterwards, a further increase of the COP concentration results in a continuous increase of the modulus. We thus see that the viscoelastic behaviour—in this case the storage modulus with its plateau, maximum and minimum—reflects the phase diagram and the morphology of the phases involved.

In connection with the results reported above, we have also studied effects of annealing time on the modulus E_b determined in three-point bending. A curve showing these effects for a sample with 50 wt% COP is provided in Figure 12. It is clear that longer annealing between 210 and 220°C increases the modulus. The results can be explained again in terms of PC crystallization; the PC concentration is sufficient for it to occur. The annealing temperature is important here, since we are below the onsets of transesterification and thermal degradation. The modulus increase effect is particularly pronounced at low temperatures. Clearly, for high temperatures, bringing the sample to the temperature of measurement is by itself tantamount to annealing. We show a curve of the E_b modulus as a function of concentration in

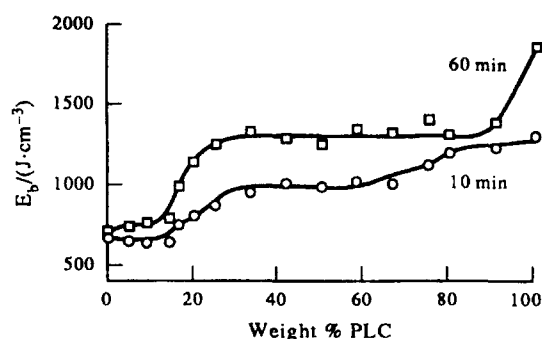


Figure 13 Bending modulus E_b of blends as a function of concentration, determined at 20°C with pendulum d.m.t.a. for samples prepared as in Figure 12

Figure 13. The curve confirms once again the role of annealing.

Returning now to the problem defined in the Introduction, we conclude the following: adding say 18% of the PLC to our EP, we obtain approximately the same reinforcement as adding 80% PLC. The modulus serves here as the measure of reinforcement. The very wide central plateau of the modulus can be clearly connected to the fall of the glass transition temperature T_g of the PC-rich phase visible in the phase diagram in Figure 3 (the border between regions VI, X and XI). In other words, when the phase diagram shows miscibility of an EP with a PLC, mechanical reinforcement of the EP is to be expected. Even more limited studies, in our case of the glass transition temperatures (Figure 2, Figures 4–6), lend themselves to the same conclusion.

The question asked at the end of the Introduction can now be answered. The intelligent processing postulated acquires a firm foundation. The mechanical reinforcement of an engineering polymer with a relatively low concentration of a PLC is possible in our system—and can be predicted on the basis of the respective phase diagram. Both equilibrium and long-living non-equilibrium phases have to be taken into account.

ACKNOWLEDGEMENTS

Financial support was provided by the Robert A. Welch Foundation, Houston, TX (Grant no. B-1203) and also by the Deutsche Forschungsgemeinschaft, Bonn (to M.H.). An equipment grant from the Perkin–Elmer Corp., Norwalk, CT, is appreciated. Dr Frank Schubert participated in the experimental work at the University of Duisburg and Messrs Kelly R. Degler and Rogelio F. Rodriguez at the University of North Texas (UNT). Comments on the manuscript kindly provided by Dr Nandika Anne D'Souza of UNT and also by a referee were helpful.

REFERENCES

- Krause, S. J., Haddock, T., Price, P. G., Lehnert, P. G., O'Brien, J. F. and Helminiak, T. E. *J. Polym. Sci.* 1986, **24**, 1991
- Brostow, W., Dziemianowicz, T. S., Romanski, J. and Werber, W. *Polym. Eng. Sci.* 1988, **28**, 785
- Husman, G., Helminiak, T., Adams, W., Wiff, D. and Benner, C. *Am. Chem. Soc. Symp. Series* 1980, **132**, 203

- Hwang, W.-F., Wiff, D. R., Benner, C. L. and Helminiak, T. E. *J. Macromol. Sci., Phys.* 1983, **B22**, 231
- Brostow, W. *Kunststoffe* 1988, **78**, 411
- Witt, W. *Kunststoffe* 1988, **78**, 795
- Brostow, W. *Polymer* 1990, **31**, 979
- Brostow, W. in 'Liquid Crystalline Polymers: From Structures to Applications' (Ed. A. A. Collyer), Elsevier Applied Science, London, New York, 1992, Ch. 1
- Siegmann, A., Dagan, A. and Kenig, S. *Polymer* 1985, **26**, 1325
- Kiss, G. *Polym. Eng. Sci.* 1987, **27**, 410
- Kiss, G. D. and Wong, R. G. *Proc. Ann. Tech. Conf. Soc. Plast. Engrs* 1987, **47**, 1708
- Groeninckx, G. and Crevecoeur, G. *Bull. Soc. Chim. Belg.* 1990, **99**, 1031
- Groeninckx, G. and Crevecoeur, G. *Polym. Eng. Sci.* 1990, **30**, 532
- Groeninckx, G. and Crevecoeur, G. *Polym. Compos.* 1992, **13**, 244
- Engberg, K., Knutsson, A., Werner, P.-E. and Gedde, U. W. *Polym. Eng. Sci.* 1990, **30**, 1620
- La Mantia, F. P., Valenza, A., Paci, M. and Magagnini, P. L. *Polym. Eng. Sci.* 1990, **30**, 7
- La Mantia, F. P. and Valenza, A. *Makromol. Chem., Symp.* 1990, **38**, 183
- Valenza, A., La Mantia, F. P., Paci, M. and Magagnini, P. L. *Int. Polym. Process.* 1991, **6**, 247
- Seppälä, J., Heino, M. T. and Kapanen, C. *J. Appl. Polym. Sci.* 1992, **44**, 1051
- Heino, M. T. and Seppälä, J. V. *J. Appl. Polym. Sci.* 1992, **44**, 2185
- Heino, M. T. and Seppälä, J. V. *Polym. Bull.* 1993, **30**, 353
- Golovoy, A., Kozłowski, M. and Narkis, M. *Polym. Eng. Sci.* 1992, **32**, 854
- La Mantia, F. P., Valenza, A. and Magagnini, P. L. *J. Appl. Polym. Sci.* 1992, **44**, 1257
- Hsu, C.-S. and Chen, L.-B. *Mater. Chem. Phys.* 1993, **34**, 28
- Menczel, J. and Wunderlich, B. *J. Polym. Sci., Phys.* 1980, **18**, 1433
- Menczel, J. and Wunderlich, B. *Polymer* 1981, **22**, 778
- Meesiri, W., Menczel, J., Gaur, U. and Wunderlich, B. *J. Polym. Sci., Phys.* 1982, **20**, 719
- Brostow, W., Dziemianowicz, T. S., Hess, M. and Kosfeld, R. *Mater. Res. Soc. Symp.* 1990, **171**, 177
- Brostow, W. and Hess, M. *Mater. Res. Soc. Symp.* 1992, **255**, 57
- Brostow, W., Hess, M. and López, B. L. *Macromolecules* 1994, **27**, 2262
- Flory, P. J. *Proc. Royal Soc. A* 1956, **234**, 60, 73
- Abe, A. and Flory, P. J. *Macromolecules* 1978, **11**, 1122
- Flory, P. J. and Ronca, G. *Mol. Cryst. Liq. Cryst.* 1979, **54**, 289, 311
- Matheson Jr, R. R. and Flory, P. J. *Macromolecules* 1981, **14**, 954
- Matheson Jr, R. R. *Macromolecules* 1986, **19**, 1286
- Jonah, D. A., Brostow, W. and Hess, M. *Macromolecules* 1993, **26**, 76
- Blonski, S., Brostow, W., Jonah, D. A. and Hess, M. *Macromolecules* 1993, **26**, 84
- Brostow, W. and Walasek, J. *Macromolecules* 1994, **27**, 2923
- Brostow, W., Sterzynski, T. and Triouleyre, S. *Polymer* 1996, **37**, 1561
- Brostow, W., Kaushik, B. K., Mall, S. B. and Talwar, I. M. *Polymer* 1992, **33**, 4687
- Brostow, W. and Samatowicz, D. *Polym. Eng. Sci.* 1993, **33**, 581
- Illers, K. H. and Breuer, H. *J. Colloid Sci.* 1963, **18**, 1
- Sawyer, L. C. and Jaffe, M. *J. Mater. Sci.* 1986, **21**, 1897
- Schubert, F. *Doctoral thesis*, University of Duisburg 1989
- Wolff, D., Cackovic, H., Krüger, H., Rübner, J. and Springer, J. *Liq. Crystals* 1993, **14**, 917
- Kühnpast, K., Springer, J., Scherowsky, G., Gießelmann, F. and Zugenmaier, P. *Liq. Crystals* 1993, **14**, 861
- Davidson, P., Kühnpast, K., Springer, J. and Scherowsky, G. *Liq. Crystals* 1993, **14**, 901
- López, B. L. *PhD Dissertation*, University of North Texas, Denton, 1994
- Yoon, D. Y., Masciocci, N., Depero, L. E., Viney, C. and Parrish, W. *Macromolecules* 1990, **23**, 1793
- Brostow, W. and Corneliussen, R. D. in 'Failure of Plastics' (Eds W. Brostow and R. D. Corneliussen), Hanser Publishers, Munich–Vienna–New York, 1986, Ch. 1

- 51 Kosfeld, R., Hess, M. and Friedrich, K. *Mater. Chem. Phys.* 1987, **18**, 93
- 52 Guan, G., Wang, H., Chang, Y., Zhou, H. and Sun, T. *J. China Text. Univer.* 1991, **17** (3), 1; quoted after *Ref. Zh. Khim. VMS* 1992, **10C**, 19
- 53 Kyu, T. and Zhuang, P. *Polym. Commun.* 1988, **29**, 99
- 54 Takayanagi, M., Ogata, T., Morikawa, M. and Kai, T. *J. Macromol. Sci., Phys.* 1980, **B17**, 591
- 55 Brostow, W. 'Science of Materials', John Wiley & Sons, New York-London, 1979; Brostow, W. 'Einstieg in die moderne Werkstoffwissenschaft', Carl Hanser Verlag, München-Wien, 1985
- 56 Blonski, S. and Brostow, W. *J. Chem. Phys.* 1991, **95**, 289